NIH-PA Author Manuscript

Treatment of Vestibular Schwannoma Cells with ErbB Inhibitors

Matthew L. Bush, M.D.[1,Φ], **Sarah S. Burns, B.A.**[1,2], **Janet Oblinger, Ph.D.**[1,2], **Sholpan Davletova, Ph.D.**[1,2], **Long-Sheng Chang, Ph.D.**[1,2,3], **D. Bradley Welling, M.D., Ph.D.**[1,*], and **Abraham Jacob, M.D.**[1,*,Ψ]

[1]Department of Otolaryngology-Head and Neck Surgery, The Ohio State University Eye and Ear Institute, Columbus, Ohio, USA

[2]Center for Childhood Cancer, The Research Institute at Nationwide Children's Hospital, Columbus, Ohio, USA

[3]Department of Pediatrics, The Ohio State University, Columbus, Ohio, USA

Abstract

Hypothesis—Aberrant phosphorylation of ErbB family receptor tyrosine kinases (RTK) in human vestibular schwannomas (VS) renders them susceptible to growth suppression by RTK inhibitors.

Background—Recent evidence has implicated increased ErbB family receptor tyrosine kinase signaling in VS tumorigenesis; however, the characterization of ErbB receptor activity and the chemotherapeutic potential of RTK inhibitors in VS treatment have not been fully explored.

Methods—To confirm phosphorylation of ErbB receptors in VS, protein extracts from paired VS tumor-vestibular nerve samples were examined using phospho-RTK arrays. ErbB receptor phosphorylation was similarly examined in cultured schwannoma cells, normal Schwann cells, and VS tumor tissues by Western blotting. Also, VS tumor sections were immunostained for members of the ErbB receptor family. The effects of RTK inhibitors on ErbB phosphorylation and cell proliferation were assessed in schwannoma cells following EGFR inhibitor (Erlotinib) and EGFR/ErbB2 inhibitor (Lapatinib) treatment.

Results—VS tumor tissues consistently demonstrated higher levels of phosphorylated ErbB3 compared with paired vestibular nerves. However, cultured VS, malignant schwannoma, and normal Schwann cells demonstrated EGFR phosphorylation. Immunohistochemistry confirmed high expression of ErbB3 in a series of VS tumor sections. Erlotinib inhibited schwannoma cell proliferation with an IC_{50} value of 2.5 micromolar, while Lapatinib was less potent for growth inhibition. Erlotinib treatment resulted in a decrease of multiple phospho-ErbB receptors in schwannoma cells.

Conclusions—VS variably express activated ErbB receptors with consistently higher levels of phospho-ErbB3 expression relative to paired vestibular nerve samples. Chemotherapeutic targeting of ErbB3 may be a novel means of inhibiting VS growth.

Conflict of interest: No conflicts of interest are declared.

Keywords

Vestibular schwannoma; NF2; EGFR; ErbB2; ErbB3; ErbB4; receptor tyrosine kinase; Erlotinib; Lapatinib

Introduction

Vestibular schwannomas (VS) are nerve sheath tumors that originate from Schwann cells of the vestibulocochlear nerve. These tumors are caused by mutations in the *Neurofibromatosis 2* gene (*NF2*), which encodes the tumor suppressor protein, merlin (1–3). Most tumors are unilateral and sporadic; however, germ-line *NF2* mutations result in formation of bilateral vestibular schwannomas, frequently seen in patients with neurofibromatosis type 2 (NF2). While VS are histologically benign, they cause hearing loss, tinnitus, cranial nerve dysfunction, balance abnormalities (4–7), and when large enough to compress the brainstem, stroke and death can occur (8).

Current treatment options for VS include surgical excision and stereotactic radiation. At this time, no chemotherapeutic options approved by the United States Food and Drug Administration (FDA) are available. Therefore, the development of a low-morbidity, medical option for VS patients with sporadic and NF2-associated tumors is an urgent clinical need. Deregulated growth-promoting, intracellular signaling pathways in vestibular schwannomas represent potential therapeutic targets. The ErbB family of receptor tyrosine kinases (RTKs), including epidermal growth factor receptor (EGFR), ErbB2/HER2, ErbB3, and ErbB4, is a structurally-related family of trans-membrane RTKs. These receptors are known to play a role in Schwann cell differentiation and proliferation (9–12). Upon ligand binding, the ErbB receptors transition from inactive monomers to active homodimers or heterodimers with other members of the ErbB family. This dimerization stimulates its protein-tyrosine kinase activity and initiates signal transduction, principally via the MAPK, AKT/PI3K, and JNK pathways (13). Merlin's tumor suppressor function is due, at least in part, to regulation of receptor trafficking at the plasma membrane in response to cell:cell contact (14, 15). For merlin-deficient fibroblasts, osteoblasts, and liver-derived epithelial cells, EGFR activation has been found to correlate with cell proliferation (14). In vestibular schwannomas, ErbB2 and ErbB3 exhibit strong proliferative signaling. ErbB2 does not bind to any ligands (16), and is the most common heterodimer partner for other ErbB receptors (17, 18). ErbB3 lacks tyrosine kinase function and must also heterodimerize to transduce signals in cells (19–21). While recent studies have shown that the ErbB-family RTKs are expressed in both vestibular nerves and vestibular schwannomas (21–23), direct comparison of ErbB receptor activation using paired vestibular schwannoma and normal vestibular nerve from the same patient has not yet been performed.

At the recent consensus conference on NF2 clinical trials, ErbB receptor inhibitors were identified as promising pharmacological agents for therapeutic development (24). Current FDA-approved RTK inhibitors function by blocking ligand-binding to the receptor (e.g., monoclonal antibodies) or by inhibiting tyrosine kinase function downstream of the ligand. Erlotinib (Roche, Nutley, NJ, USA) targets kinase activity of EGFR by binding to its ATP binding site (25, 26) while Lapatinib (GlaxoSmithKline, London, UK) inhibits the ATP-binding sites of both EGFR and ErbB2 (27). The objective of this research was to characterize the expression and phosphorylation of the ErbB family of RTKs in vestibular schwannoma tumor and normal nerve tissues as well as cultured schwannoma cells. Also, we assessed both the growth-inhibitory as well as molecular target effects of Erlotinib and Lapatinib in cultured schwannoma cells.

Materials and Methods

Chemical compounds

Lapatinib di-p-toluenesulfonate salt (L-4804) and erlotinib HCl salt (E-4007) were obtained from LC Labs, Woburn, MA, and were dissolved in DMSO as a stock solution of 10 mM (lapatinib) and 20 mM (erlotinib).

Human Tissue Acquisition and Generation of Primary VS Cell Cultures

Our Institutional Review Board approved the Human Subjects Protocols for the acquisition of surgically-removed VS specimens and uninvolved vestibular nerves from patients. The control vestibular nerve for each tumor/nerve pair was harvested adjacent to the vestibular schwannoma within the internal auditory canal. A clinical neuropathologist confirmed the diagnosis of vestibular schwannomas. A portion of vestibular schwannomas and paired uninvolved vestibular nerves were snap frozen in liquid nitrogen and stored at −80°C. Fresh tumor tissues were placed in Dulbecco's Modified Eagle's medium (DMEM) (Invitrogen, Carlsbad, CA) and promptly transported to the laboratory. Specimens were minced and dissociated with 0.6 U/mL collagenase (Serva, Heidelberg, Germany) and 0.125 U/mL dispase (Invitrogen) for 3–5 hours in a 37°C humidified incubator. The dissociated tissue fragments were then triturated, spun down, and grown in poly-D-lysine–laminin (PDLL)-coated dishes containing DMEM supplemented with 10% fetal bovine serum (FBS), 10 ng/mL recombinant human NRG1-β1/HRG1-β1 EGF domain (heregulin, R&D Systems, Minneapolis, MN), and 0.2 µM forskolin (Sigma, St. Louis, MO). Human malignant schwannoma HMS-97 cells were grown in noncoated plates containing DMEM/10%FBS.

For preparing primary Schwann cells (SCs), femoral nerves from organ donors (supplied by Lifeline of Ohio) were was carefully dissected away from the connective tissues and the fascicles, and then incubated in DMEM, 10% FBS, and 1x antibiotic/antimycotic solution (Invitrogen) for 1–2 weeks at 37°C to allow Wallerian degeneration. Degenerated nerves were dissociated with 0.125 U/mL collagenase/0.6 U/mL dispase overnight at 37°C, triturated and spun down. Normal SCs were then cultured on PDLL-coated plates and fed with DMEM/10% FBS supplemented with heregulin and forskolin in the same concentrations as schwannoma cultures.

Receptor Tyrosine Kinase Arrays and Western Blot Analysis

The Human Phosphorylated Receptor Tyrosine Kinase (RTK) Array (R&D Systems) was used to determine the phosphorylation status of 42 different RTKs in three pairs of VS-vestibular nerve tissues (AXL, DTK, EGFR, ErbB2, ErbB3, ErbB4, EphA1, EphA2, EphA3, EphA4, EphA6, EphA7, EphB1, EphB2, EphB4, EphB6, FGFR1, FGFR2α, FGFR3, FGFR4, FLT3, HGFR, Insulin R, IGFR1, MER, MSPR, PDGFRα, PDGFRβ, SCFR, M-CSFR, C-RET, ROR1, ROR2, Tie-1, Tie-2, TrkA, TrkB, TrkC, MuSK, VEGFR1, VEGFR2, and VEGFR3). Tumor and nerve samples were homogenized in lysis buffer (20 mM Tris, 150 mM NaCl, 1 mM EDTA, 1 mM EGTA, 1% Triton X-100, 2.5 mM sodium pyrophosphate, pH 7.5) supplemented with protease and phosphatase inhibitors (1 mM PMSF, 1 mM sodium orthovanadate, 1X protease inhibitor cocktail [Sigma-Aldrich], and 0.5 µg/ml pepstatin A [Roche, Indianapolis, IN]). Soluble proteins were isolated with centrifugation and protein concentrations were assayed using the microBCA kit (Pierce, Rockford, IL). An equal amount (300 µg) of protein lysates was applied to each phospho-RTK array membrane, according to the manufacturer's instructions. Each membrane possesses negative controls spots to identify non-specific binding, and all membranes were found to have the appropriate presence or absence of signal for the positive and negative controls (Figure 1). The expression level of each phospho-RTK in each VS and the paired vestibular nerve was detected by enhanced chemiluminescence (ECL; GE Healthcare). Pixel

density from densitometry was calculated by subtracting an averaged background signal of the negative control spots from the averaged signal of the duplicate spots representing each RTK. Corresponding signals of paired tumor/vestibular nerve arrays were compared.

For phospho-RTK array analysis of cultured VS, HMS-97 schwannoma, and Schwann cells, an equal amount (300 μg) of cell lysates was used as described above. The *in vitro* effect of erlotinib treatment was also assessed in cultured VS and HMS-97 cells with or without erlotinib treatment (5 μM) for 24 hours.

For immunoblotting, subconfluent cells were collected and lysed in lysis buffer supplemented with protease and phosphatase inhibitors. Lysates were sonicated for 10 seconds, and the total protein content was assayed using the microBCA kit (Pierce, Rockford, IL). Equal amounts of cell lysates were resolved by SDS-PAGE and transferred to PVDF membranes, followed by probing with antibodies against total EGF Receptor (No. 4267; Cell Signaling Technology), phospho-EGFR [Tyr992] (No. 2235; Cell Signaling Technology), total HER2/ErbB2 (No. 4290; Cell Signaling Technology), total ErbB3 (sc-285; Santa Cruz Biotechnology), and total ErbB4 (sc-71071; Santa Cruz Biotechnology). An antibody against α-tubulin (sc-32293; Santa Cruz Biotechnology) was used to determine equal protein loading. Similarly, VS tumor and normal nerve tissues were homogenized in lysis buffer and analyzed for total EGFR, phospho-EGFR and α-tubulin.

Cell Proliferation Assay

Cell proliferation was assessed by using the CellTiter 96 AQueous One Solution Cell Proliferation Assay (Promega, Madison, WI), according to the manufacterer's instructions. Cells were plated in 96-well plates at 4,000 cells per well. PDLL-coated plates were used for VS and noncoated plates were used for HMS-97 cells. After 24 hours, cells were treated with various concentrations of Erlotinib or Lapatinib with DMSO as a vehicle control at 37°C for 72 hours. After treatment, 20 μL of the MTS assay reagent was added to each well and incubated for 1–3 hours. Since only viable cells will induce a color change, the amount of bio-reduced formazan was estimated by measuring the absorbance at 490 nm. Each treatment condition had six replicates and each experiment was repeated using subsequent cell passages. The untreated wells represented the baseline of viable cells and designated as 100%. The percentage of viable cells for each drug treatment compared with the untreated wells was plotted against the concentration of drug. The mean percentage with standard deviations were calculated. These data were used for qualitative and descriptive purposes and no further statistical analyses were performed between individual tumors or different inhibitors. The IC_{50} value, defined as the drug concentration at which the mean of viable cells decreased to 50%.

Vestibular Schwannoma ErbB receptor Immunohistochemistry

Paraffin-embedded sections from six vestibular schwannomas were deparaffinized in xylene followed by antigen retrieval in citrate buffer (pH 6.0) at 121°C for 30 minutes in a pressure cooker. Samples were treated with 3% hydrogen peroxide, blocked in Superblock (Scytek Laboratories, Logan, UT) for 10 minutes at room temperature, and stained with the following primary antibodies overnight at 4°C: EGFR at 1:50 dilution, HER2/ErbB2 at 1:400 dilution, ErbB3 at 1:250 dilution, and ErbB4 at 1:125 dilution. Following washing, sections were incubated with an anti-polyvalent, biotinylated secondary antibody and streptavidin/horseradish peroxidase (Scytek Laboratories, Logan, UT) for 20 minutes at room temperature. Staining was detected using AEC (3-amino-9-ethylcarbazole) (Scytek Laboratories, Logan, UT), and hematoxylin was used as a counterstain. Tissue sections treated by the same procedure but without incubation with a primary antibody were used as

negative controls. Glioblastoma and breast cancer tissue sections were used as positive controls.

Results

Vestibular Schwannoma Tumors Display Higher Expression of Phospho-ErbB3 than Paired Vestibular Nerves

Three paired VS and vestibular nerve samples were analyzed with RTK arrays. All VS were sporadic tumors and maximal tumor diameters measured from 1.4 ~ 2.6 cm in size. The first tumor-nerve pair exhibited multiple phosphorylated RTKs (Figure 1A). Pixel density analysis by densitometry provided a quantitative comparison between the tumor and nerve pair (Figure 1B). All four phosphorylated ErbB receptors were detected in VS and normal nerves; however, the levels of phosphorylated ErbB2, ErbB3, and ErbB4 were significantly higher in the tumor specimen as compared with the paired normal vestibular nerve. Also, fibroblast growth factor receptor-2α (FGFR-2α), insulin receptor, macrophage-stimulating protein receptor (MSPR), platelet-derived growth factor receptor-β (PDGFR-β), C-RET, and Ephrin type-A4 receptor (EphA4) were among the receptors that were elevated in the tumor, in comparison with the paired vestibular nerve. The significance for these elevated phosphor-RTKs in VS is presently unclear. Tumor-nerve pair #2 expressed phosphorylated ErbB receptors, insulin receptor, and PDGFR-β (Figure 1C); however, only phospho-ErbB3 was elevated in the tumor, compared with the paired vestibular nerve (Figure 1D). Tumor-nerve pair #3 (Figure 1E) displayed a similar pattern as pair #2 with a high level of phospho-ErbB3 in the tumor (Figure 1F). The ratios of phosphorylated ErbB3 receptor in the tumor-nerve pairs were 1.9 ~ 12.8 times (higher expression in VS than in their corresponding vestibular nerve) (Table 1). In addition, we confirmed the expression of total EGFR protein in VS tumor and vestibular nerve specimens. We readily detected EGFR protein in both superior and inferior vestibular nerves and two out of four VS tumors (Figure 2). Together, these data indicate that VS frequently display phosphorylation of one or multiple ErbB receptors, most significantly phospho-ErbB3.

Cultured Schwannoma Cells Express Elevated Levels of Phospho-EGFR

To examine whether cultured VS and Schwann cells exhibited a similar expression profile of phospho-RTKs, we prepared primary cultures of VS cells and Schwann cells from normal nerves and analyzed their RTK phosphorylation status (Figure 3). For comparison, we also analyzed phospho-RTK expression in human malignant schwannoma HMS-97 cells. Similar to VS tumor tissues, we detected phospho-ErbB3 in cultured VS cells. However, we also detected a high level of phospho-EGFR in these cultured tumor cells. Also, while phospho-EGFR was seen in cultured Schwann cells, little or no phosphorylated ErbB2, ErbB3, and ErbB4 were observed. Although HMS-97 cells showed robust expression of phospho-EGFR, they also expressed high levels of phosphorylated ErbB2 and ErbB4.

To confirm the expression pattern of ErbB receptors, we performed Western blot analysis. Intriguingly, two out of three VS cultures expressed substantially higher levels of total EGFR than normal Schwann cells (Figure 4A). Expression of total ErbB2, ErbB3, and ErbB4 were similar for cultured VS and Schwann cells with some variations. To examine whether the levels of EGFR expression in cultured VS cells correlated with its phosphorylation status, Western blotting for a phospho-EGFR(Tyr992) was performed. Consistently, we detected higher levels of this EGFR phosphorylation in VS cultures 1 and 3, compared to normal Schwann cells (Figure 4B).

Collectively, these results suggest that culture conditions may selectively activate EGFR in schwannoma and Schwann cells.

Immunohistochemical Analysis of Vestibular Schwannomas Confirms Expression of ErbB Receptors

A series of six VS tumors was examined for ErbB receptor protein expression by immunohistochemistry (Figures 5A–C). The characteristics of these tumors are summarized in Table 2. One tumor was obtained from an NF2 patient while the other five were sporadic in nature. Maximal tumor diameter ranged from 1.8 ~ 2.3 cm, and three tumors exhibited areas of cystic degeneration. All tumors expressed several ErbB receptors with ErbB3 having consistently higher expression in all tumors. A cystic tumor (tumor #3 in Table 2) displayed marked expression of ErbB2, ErbB3, and ErbB4 (Figures 5A and 5B). A sixth VS tumor, which was also a cystic tumor, showed modest EGFR expression; however, ErbB3 expression was clearly demonstrated (Figure 5C). We also stained normal human sciatic nerve sections. While ErbB3 expression was readily detected, much lower levels of EGFR and ErbB2 were observed (Figure 5D). For positive controls, we detected strong EGFR expression and a modest level of ErbB2 in glioblastoma tumor sections and intense ErbB3 expression and a moderate expression level of ErbB4 in breast cancer sections (Figure 5E). Clearly, the detection of ErbB3 and ErbB4 expression in breast cancer tissues can be easily distinguished from negative stroma tissues (Figure 5F). Further, immunostaining of a VS tumor section omitting the primary antibody displayed negative staining (Figure 5G).

Inhibition of ErbB RTK Activity Decreases Schwannoma Cell Proliferation

To determine whether ErbB inhibitors could decrease schwannoma cell proliferation, we treated primary VS and HMS-97 cells with various concentrations of Erlotinib or Lapatinib and examined cell proliferation using MTS assays (figure 4). Erlotinib inhibited VS cell proliferation in a dose-dependent manner with an IC_{50} of approximately 2.5 μM (Figure 6A). HMS-97 cells treated in a similar manner exhibited a dose-dependent inhibition of proliferation; however, the IC_{50} value could not be accurately determined due to overlapping error bars in the percentage of viable cells at concentrations greater than 2.5 μM (Figure 6B). Intriguingly, Lapatinib appeared to be less potent than Erlotinib in VS (Figure 6C) and HMS-97 cells (Figure 6D). A decrease in viable VS cells was not observed until Lapatinib concentration reached 15 μM. A similar effect was seen in HMS-97 cells treated with Lapatinib.

Erlotinib Decreases EGFR Activation in VS cells

Since Erlotinib inhibited the growth of cultured schwannoma cells, we examined the effect of drug exposure on its primary molecular target, EGFR. A primary culture of VS cells was prepared and showed preferential phospho-EGFR expression. This VS culture and HMS-97 cells were treated with 5 μM of Erlotinib for 24 hours, and the effect on receptor phosphorylation was assessed using phospho-RTK arrays. Erlotinib-treated VS cells had a noticeable decrease in phospho-EGFR (Figure 7). Treatment of HMS-97 cells, which expressed phosphorylated EGFR, ErbB2, and ErbB4, also led to a decrease in the phosphorylation of these receptors. These data suggest that Erlotinib may indirectly inhibit phosphorylation of ErbB receptor members other than EGFR at the concentration used in the study.

Discussion

Currently, no medical therapies approved by the FDA are available for sporadic and NF2-associated VS. Although observation with serial imaging, microsurgical resection, and stereotactic radiotherapy provide reasonable management options, potent, effective, and non-toxic medications that inhibit VS progression would greatly benefit VS patients. Further characterization of key signaling pathway and preclinical drug testing are vital in exploring chemotherapeutic options for VS. The current study examines the expression of total and

phosphorylated ErbB receptors and their *in vitro* response to inhibitors. We demonstrated consistently higher levels of total and phosphorylated ErbB3 in VS tumor tissues relative to paired vestibular nerves, while both phospho-EGFR and phospho-ErbB3 were elevated in cultured VS cells. Furthermore, VS cell proliferation was inhibited by ErbB receptor inhibitors, and Erlotinib exhibited higher potency of growth inhibition than Lapatinib.

The role and mechanism of ErbB-family receptors in VS development and progression has not been fully elucidated; however activation or overexpression ErbB receptors has been linked to increased Schwann cell proliferation and VS tumor formation (28–30). Many other human cancers overexpress ErbB receptors (31–35). EGFR and ErbB4 are fully functional RTKs while ErbB2 does not bind any known ligand. ErbB3 lacks independent kinase activity; however, on heterodimerization with other ErbB members, the cytoplasmic domain of phosphorylated and activated ErbB3 potently recruits PI3K to six distinct phosphotyrosine residues on ErbB3. Phospho-ErbB3 efficiently evades ligand-induced degradation (36, 37) while strongly activating the pro-growth AKT/PI3K pathway, especially when bound to ErbB2 (38). ErbB2 heterodimers are characterized by high affinity, broad specificity, and potent mitogenic signaling potential due to frequent recycling back to the plasma membrane after internalization.

To better understand merlin's relationship with RTKs in Schwann cells, Lallemand et al. (15) cultured primary murine Schwann cells derived from $Nf2^{flox2/flox2}$ mice (39, 40) and utilized adenovirus-mediated Cre expression to generate two distinct populations of Schwann cells, namely $Nf2^{+/+}$ and $Nf2^{-/-}$. While no differences were observed in growth rates between $Nf2^{+/+}$ and $Nf2^{-/-}$ Schwann cells in sub-confluent cultures, the $Nf2^{-/-}$ Schwann cells were not able to sense contact inhibition and kept growing despite confluence. $Nf2^{+/+}$ Schwann cells became senescent after five to seven passages in culture while $Nf2^{-/-}$ Schwann cells did not undergo replicative-senescence. The loss of merlin increased the abundance of ErbB2, ErbB3, insulin-like growth factor 1 receptor (IGF1R), and PDGFR-β at the plasma membrane in confluent but not sub-confluent Schwann cells. Reintroduction of merlin into $Nf2^{-/-}$ SCs reduced recycling of internalized growth factor receptors back to the plasma membrane in confluent cells. Varying the concentration of insulin, an IGF1R ligand, had no effect on the $Nf2^{-/-}$ Schwann cell phenotype, but lowering the levels of heregulin-β1, an ErbB receptor ligand, restored contact inhibition and replicative-senescence, suggesting that ErbB receptor signaling contributed directly to the deregulated growth observed in *Nf2*-deficient cells. As VS are merlin-deficient, they often display aberrant ErbB receptor signaling. Consistent with this notion, we observed elevated ErbB receptor expression, particularly ErbB3, in both VS tumor and cultured cells. However, cultured VS cells also showed high levels of phospho-EGFR expression, suggesting that culture conditions selectively enhance EGFR activation and signaling.

Studies using human tissues have found that EGFR and ErbB2 are upregulated in VS and may be targets for therapeutic intervention. Doherty and colleagues (23) demonstrated that VS upregulated EGFR in 68% and ErbB2 in 84% of specimens. EGF was upregulated in all NF2-related VS, but none of the sporadic VS, and heregulin, an ErbB ligand, was upregulated in 86% of sporadic VS but only 19% of NF2-related VS. Using cultured VS cells, Brown and Hansen (22) found that phosphorylated ErbB2 localized to lipid rafts, micro-domains in the plasma membrane that regulate receptor signaling. Our results on phosphorylated ErbB receptor expression are consistent with a recent report by Ammoun et al. who showed elevated expression of multiple phosphorylated ErbB-family receptors in VS tumors (41).

As reported previously, we demonstrated activation of multiple RTKs in VS compared to paired vestibular nerves. Although the number of tumor/nerve pairs used in this study is

limited, our data represents a unique within-patient comparison that has not been described previously. Based on the current evidence, a larger study to compare paired samples is warranted. Interestingly, although all three sporadic VS tumors exhibited some variability of phosphor-ErbB receptor expression, they consistently expressed total and phospho-ErbB3. In addition, we observed that one NF2 tumor (VS1 from Figure 5) had expression of all four ErbB members with prominent ErbB3 staining, consistent with the results from phospho-RTK arrays and Western blot analysis.

In addition to phospho-ErbB receptors, we identified elevated expression of phosphorylated FGFR-2α, insulin receptor, macrophage-stimulating protein receptor (MSPR), PDGFR-β, C-RET, and EphA4 in VS. Activation of FGFR and PDGFR has been linked to VS growth and progression (43, 44). While the remaining phospho-RTKs have been linked to human cancers, their roles in VS tumorigenesis are presently unknown.

Most of the currently-available drugs that inhibit the ErbB family of receptors target EGFR and ErbB2. Inhibition of EGFR with Gefitinib has been shown to induce a cytostatic effect in merlin-deficient cells (14). Trastuzumab, a monoclonal antibody to ErbB2, has been shown to inhibit growth of VS cells (45). Clinical use of Erlotinib was reported in one patient with VS, and a reduction of tumor volume was observed in this short-term study (46). However, in a subsequent study with 11 NF2 patients, only a small subset of Erlotinib-treated patients had prolonged stable disease (47). A clinical trial for Lapatinib is ongoing but the results have not been reported. Our data showed that Lapatinib was less potent than Erlotinib in suppressing schwannoma cell proliferation. While the reason for this finding is presently not understood, it is plausible that inhibition of ErbB2 by Lapatinib may result in up-regulation of ErbB3 as reported by Garrett et al. (42). Inhibition of both ErbB2 and ErbB3 is likely to be a more effective therapeutic strategy in VS. We are presently investigating this possibility.

It should be mentioned that the response of cells to ErbB inhibitors may be cell type and context-dependent. Frolov et al. (48) found that ErbB3:EGFR heterodimerization induced activation of the PI3K/AKT pathway, and ErbB3 expression increased susceptibility of pancreatic cancer cells to Erlotinib treatment. Liles et al. (49) found that combined treatment with MM-121, an ErbB3 monoclonal antibody, and Erlotinib gave rise to a greater degree of tumorigenesis inhibition in pancreatic ductal adenocarcinoma cells that depend on ErbB3-mediated signaling. In breast cancer cells that are driven by ErbB2 activation, the presence of ErbB3 has been shown to promote growth and may overcome RTK inhibition by EGFR and ErbB2 inhibitors (50). Furthermore, ErbB inhibitor efficacy appears to be closely linked to ErbB3 transphosphorylation. We (51) previously reported activation of the PI3K/AKT pathway in VS cells. It is tempting to speculate that the interaction with ErbB3 may be significant in this process. Although Erlotinib is thought to primarily target EGFR, our data showed that Erlotinib could decrease phosphorylation of multiple ErbB receptors in schwannoma cells. It will be interesting to examine whether this decrease is due to the transphosphorylation activity of EGFR.

This study supports a need for further development of a more potent ErbB receptor inhibitor and a combined treatment strategy for VS. ErbB receptor inhibitors have the advantage of a more favorable clinical side effect profile than other chemotherapeutics in long-term dosing (52–55), which would be required in patients with VS. A safe and effective medical treatment, which preserves neurologic function while inhibiting VS tumor growth, would be most welcomed by the patients, their loved ones and their treating physicians alike.

Conclusion

VS tumor tissues exhibited elevated expression of multiple phospho-ErbB receptors, particularly ErbB3, compared with paired vestibular nerves. Cultured schwannoma cells selectively activated EGFR. Treatment of schwannoma cells with Erlotinib resulted in a dose-dependent inhibition of proliferation with a concomitant decrease in the activation of multiple ErbB receptors. Treatment with Lapatinib gave rise to a more modest effect of growth inhibition. Further investigation into the complex interactions among ErbB members in VS may open a new avenue for the clinical treatment of these debilitating tumors.
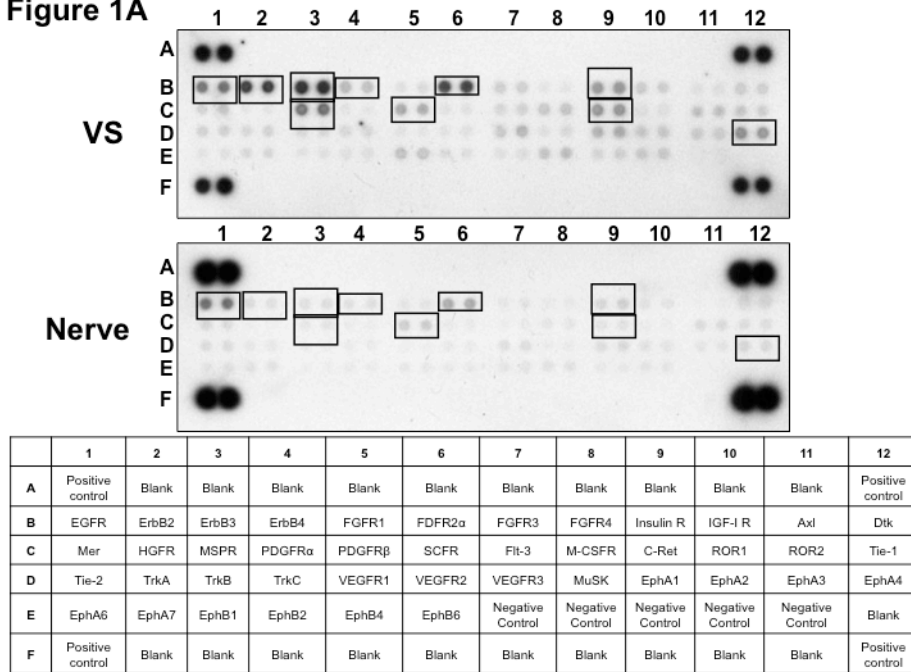
Acknowledgments

Bibliography

1. Rouleau GA, et al. Alteration in a new gene encoding a putative membrane-organizing protein causes neuro-fibromatosis type 2. Nature. 1993; 363:515–521. [PubMed: 8379998]

2. Trofatter JA, et al. A novel moesin-, ezrin-, radixin-like gene is a candidate for the neurofibromatosis 2 tumor suppressor. Cell. 1993; 72:791–800. [PubMed: 8453669]

3. Welling DB, Packer MD, Chang L-S. Molecular studies of vestibular schwannomas: a review. Curr Opin Otolaryngol Head Neck Surg. 2007; 15(5):341–6. [PubMed: 17823551]

4. Matthies C, Samii M. Management of 1000 vestibular schwannomas (acoustic neuromas): clinical presentation. Neurosurgery. 1997; 40:1–9. discussion in p9–10. [PubMed: 8971818]

5. Sauvaget E, et al. Sudden sensorineural hearing loss as a revealing symptom of vestibular schwannoma. Acta Otolaryngol. 2005; 125:592–595. [PubMed: 16076707]

6. Nageris BI, Popovtzer A. Acoustic neuroma in patients with completely resolved sudden hearing loss. Ann Otol Rhinol Laryngol. 2003; 112:395–397. [PubMed: 12784975]

7. Kameda K, et al. Effect of tumor removal on tinnitus in patients with vestibular schwannoma. J Neurosurg. 2010; 112:152–157. [PubMed: 19480542]

8. Evans DG. Neurofibromatosis type 2 (NF2): a clinical and molecular review. Orphanet J Rare Dis. 2009; 4:16. [PubMed: 19545378]

9. Dong Z, Brennan A, Liu N, et al. Neu differentiation factor is a neuron-glia signal and regulates survival, proliferation, and maturation of rat Schwann cell precursors. Neuron. 1995; 15:585–596. [PubMed: 7546738]

10. Michailov GV, Sereda MW, Brinkmann BG, et al. Axonal neuregulin-1 regulates myelin sheath thickness. Science. 2004; 304:700–703. [PubMed: 15044753]

11. Maurel P, Salzer JL. Axonal regulation of Schwann cell proliferation and survival and the initial events of myelination requires PI3-kinase activity. J Neurosci. 2000; 20:4635–4645. [PubMed: 10844033]

12. Levi ADO, Bunge RP, Lofgren JA, et al. The influence of heregulins on human Schwann cell proliferation. J Neurosci. 1995; 15:1329–1340. [PubMed: 7869101]

13. Burden S, Yarden Y. Neuregulins and their receptors: a versatile signaling module in organogenesis and oncogenesis. Neuron. 1997; 18:847–855. [PubMed: 9208852]

14. Curto M, Cole BK, Lallemand D, Liu CH, McClatchey AI. Contact-dependent inhibition of EGFR signaling by Nf2/Merlin. J Cell Biol. 2007; 177:893–903. [PubMed: 17548515]

15. Lallemand D, Manent J, Couvelard A, et al. Merlin regulates transmembrane receptor accumulation and signaling at the plasma membrane in primary mouse Schwann cells and in human schwannomas. Oncogene. 2009; 28:854–865. [PubMed: 19029950]
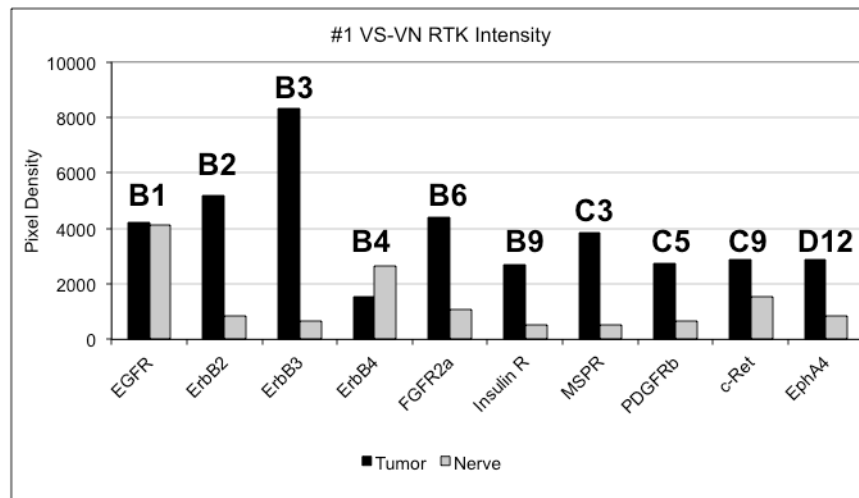
16. Klapper LN, Glathe S, Vaisman N, Hynes NE, Andrews GC, Sela M, Yarden Y. The ErbB-2/ HER2 oncoprotein of human carcinomas may function solely as a shared coreceptor for multiple stroma-derived growth factors. Proc Natl Acad Sci USA. 1999; 96:4995–5000. [PubMed: 10220407]

17. Yamamoto T, Ikaawa S, Akiyama T, et al. Similarity of protein encoded by the human c-erbB-2 gene to epidermal growth factor receptor. Nature. 1986; 319:230–234. [PubMed: 3003577]

18. Hynes NE, Stern DF. The biology of erbB-2/neu/HER-2 and its role in cancer. Biochem Biophys Acta. 1994; 1198:165–184. [PubMed: 7819273]

19. Stonecypher MS, Chaudhury AR, Byer SJ, Carroll SL. Neuregulin growth factors and their ErbB receptors form a potential signaling network for schwannoma tumorigenesis. J Neuropathol Exp Neurol. 2006; 65:162–175. [PubMed: 16462207]

20. Hansen MR, Roehm PC, Chatterjee P, Green SH. Constitutive neuregulin-1/ErbB signaling contributes to human vestibular schwannoma proliferation. Glia. 2006; 53:593–600. [PubMed: 16432850]

21. Hansen MR, Linthicum FH Jr. Expression of neuregulin and activation of ErbB receptors in vestibular schwannomas: possible autocrine loop stimulation. Otol Neurotol. 2004; 25:155–159. [PubMed: 15021776]

22. Brown KD, Hansen MR. Lipid raft localization of ErbB2 in vestibular schwannoma and Schwann cells. Otol Neurotol. 2008; 29:79–85. [PubMed: 18199961]

23. Doherty JK, Ongkeko W, Crawley B, et al. ErbB and Nrg: potential molecular targets for vestibular schwannoma pharmacotherapy. Otol Neurotol. 2008; 29:50–57. [PubMed: 18199957]

24. Evans DG, Kalamarides M, Hunter-Schaedle K, et al. Consensus recommendations to accelerate clinical trials for neurofibromatosis type 2. Clin Cancer Res. 2009; 15:5032–5039. [PubMed: 19671848]

25. Press MF, Lenz HJ. EGFR, HER2 and VEGF pathways: validated targets for cancer treatment. Drugs. 2007; 67:2045–2075. [PubMed: 17883287]

26. Baselga J. Why the epidermal growth factor receptor? The rationale for cancer therapy. Oncologist. 2002; 7(suppl 4):2–8. [PubMed: 12202782]

27. Medina PJ, Goodin S. Lapatinib: A Dual Inhibitor of Human Epidermal Growth Factor Receptor Tyrosine Kinases. Clin Therapeutics. 2008; 30:1426–1447.

28. Yarden Y, Sliwkowski MX. Untangling the ErbB signaling network. Nature Rev Mol Cell Biol. 2001; 2:131–141.

29. Moasser MM. The oncogene HER2: its signalling and transforming functions and its role in human cancer pathogenesis. Oncogene. 2007; 26:6469–6487. [PubMed: 17471238]

30. Roberts PJ, Der CJ. Targeting the Raf-MEK-ERK mitogen activated protein kinase cascade for the treatment of cancer. Oncogene. 2007; 26:3291–3310. [PubMed: 17496923]

31. Slamon DJ, Godolphin E, Jones LA, Holt JA, Wong SG, Keith DE. Studies of the HER-2/neu protooncogene in human breast and ovarian cancer. Science. 1989; 244:707–712. [PubMed: 2470152]

32. Amsellem-Ouazana D, Bieche I, Tozlu S, Botto H, Debre B, Lidereau R. Gene expression profiling of ERBB receptors and ligands in human transitional cell carcinoma of the bladder. J Urol. 2006; 175:1127–1132. [PubMed: 16469638]

33. Bieche I, Onody P, Tozlu S, Driouch K, Vidaud M, Lidereau R. Prognostic value of ERBB family mRNA expression in breast carcinomas. Int J Cancer. 2003; 106:758–765. [PubMed: 12866037]

34. Junttila TT, Laato M, Vablberg T, Soderstrom KO, Visacorpi T, Isola J, Elenius K. Identification of patients with transitional cell carcinoma of the bladder overexpressing ErbB2, ErbB3, or specific ErbB4 isoforms: real-time reverse transcription-PCR analysis in estimation of ErbB receptor status from cancer patients. Clin Cancer Res. 2003; 9:5346–5357. [PubMed: 14614020]

35. Kew Y, Bell JA, Pinder SE, Denley H, Srinivasan R, Gullick WJ, Nicholson RI, Blamey RW, Ellis IO. ErbB4 protein expression in human breast cancer. Br J Cancer. 2000; 82:1163–1170. [PubMed: 10735500]

36. Baulida J, et al. All ErbB receptors other than the epidermal growth factor receptor are endocytosis impaired. J Biol Chem. 1996; 271:5251–5257. [PubMed: 8617810]
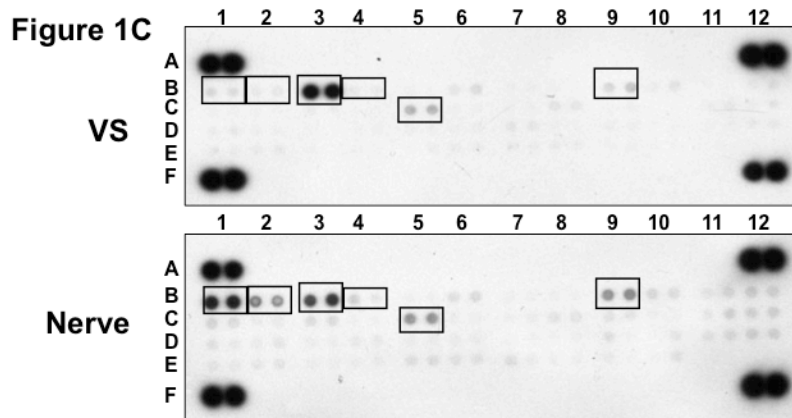
37. Waterman H, et al. The C-terminus of the kinase-defective neuregulin receptor ErbB-3 confers mitogenic superiority and dictates endocytic routing. EMBO J. 1999; 18:3348–3358. [PubMed: 10369675]

38. Wallasch C, et al. Heregulin-dependent regulation of HER2/neu oncogenic signaling by heterodimerization with HER3. EMBO J. 1995; 14:4267–4275. [PubMed: 7556068]

39. Giovannini M, et al. Conditional biallelic Nf2 mutation in the mouse promotes manifestations of human neurofibromatosis type 2. Genes Dev. 2000; 14:1617–1630. [PubMed: 10887156]

40. Manent J, et al. Magnetic cell sorting for enriching Schwann cells from adult mouse peripheral nerves. J Neurosci Methods. 2003; 123:167–173. [PubMed: 12606065]

41. Ammoun S, Cunliffe CH, Allen JC, Chiriboga L, Giancotti FG, Zagzag D, Hanemann CO, Karajannis MA. ErbB/HER receptor activation and preclinical efficacy of lapatinib in vestibular schwannoma. Neuro Oncol. 2010; 12:834–843. [PubMed: 20511180]

42. Garrett JT, Olivares MG, Rinehart C, Granja-Ingram ND, Sánchez V, Chakrabarty A, Dave B, Cook RS, Pao W, McKinely E, Manning HC, Chang J, Arteaga CL. Transcriptional and posttranslational up-regulation of HER3 (ErbB3) compensates for inhibition of the HER2 tyrosine kinase. Proc Natl Acad Sci USA. 2011; 108:5021–5026. [PubMed: 21385943]

43. Ammoun S, Flaiz C, Ristic N, Schuldt J, Hanemann CO. Dissecting and targeting the growth factor-dependent and growth factor-independent extracellular signal-regulated kinase pathway in human schwannoma. Cancer Res. 2008; 68:5236–5245. [PubMed: 18593924]

44. Nair SB, Leung HY, Ince P, Ramsden RT, Wilson JA. Fibroblast growth factor receptor expression in vestibular schwannoma. Clin Otolaryngol Allied Sci. 2000; 25:570–576. [PubMed: 11123169]

45. Clark JJ, Provenzano M, Diggelmann HR, Ningyong Xu, Hansen SS, Hansen MR. The ErbB Inhibitors Trastuzumab and Erlotinib Inhibit Growth of Vestibular Schwannoma Xenografts in Nude Mice: A Preliminary Study. Otol Neurotol. 2008; 29:846–853. [PubMed: 18636037]

46. Plotkin SR, Singh MA, O'Donnell CC, Harris GJ, McClatchey AI, Halpin C. Audiologic and radiographic response of NF2-related vestibular schwannoma to erlotinib therapy. Nat Clin Pract Oncol. 2008; 5:487–491. [PubMed: 18560388]

47. Plotkin SR, Halpin C, McKenna MJ, Loeffler JS, Batchelor TT, Barker FG 2nd. Erlotinib for progressive vestibular schwannoma in neurofibromatosis 2 patients. Otol Neurotol. 2010; 31:1135–1143. [PubMed: 20736812]

48. Frolov A, Schuller K, Tzeng CW, et al. ErbB3 expression and dimerization with EGFR influence pancreatic cancer cell sensitivity to erlotinib. Cancer Biol Ther. 2007; 6:548–554. [PubMed: 17457047]

49. Liles JS, Arnoletti JP, Kossenkov AV, et al. Targeting ErbB3-mediated stromal-epithelial interactions in pancreatic ductal adenocarcinoma. Br J Cancer. 2011; 105:523–533. [PubMed: 21792199]

50. Sergina NV, Rausch M, Wang D, Blair J, Hann B, Shokat KM, Moasser MM. Escape from HER-family tyrosine kinase inhibitor therapy by the kinase-inactive HER3. Nature. 2007; 445:437–441. [PubMed: 17206155]

51. Jacob A, Lee T, Neff BA, et al. Phosphatidylinositol 3-Kinase/AKT pathway activation in human vestibular schwannoma. Otol Neurotol. 2008; 29:58–68. [PubMed: 18199958]

52. Gril B, Palmieri D, Bronder JL, et al. Effect of lapatinib on the outgrowth of metastatic breast cancer cells to the brain. J Natl Cancer Inst. 2008; 100:1092–1103. [PubMed: 18664652]

53. Lin NU, Carey LA, Liu MC, et al. Phase II trial of lapatinib for brain metastases in patients with human epidermal growth factor receptor 2-positive breast cancer. J Clin Oncol. 2008; 26:1993–1999. [PubMed: 18421051]

54. Dhillon S, Wagstaff AJ. Lapatinib. Drugs. 2007; 67:2101–2108. discussion in p2109–2110. [PubMed: 17883289]

55. Herbst RS. Review of epidermal growth factor receptor biology. Int J Radiat Oncol Biol Phys. 2004; 59:21–26. [PubMed: 15142631]
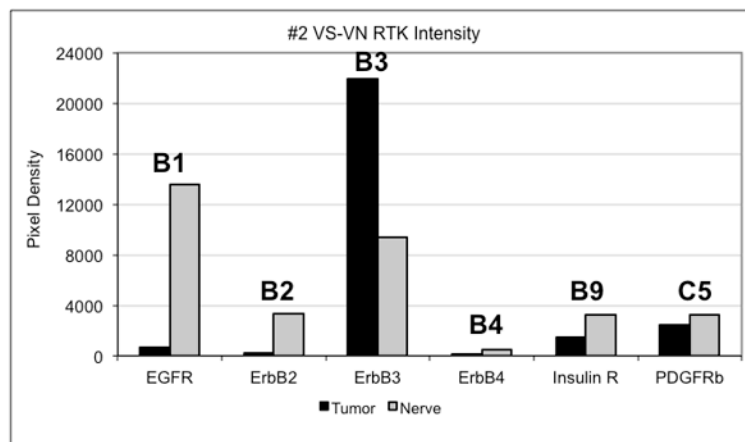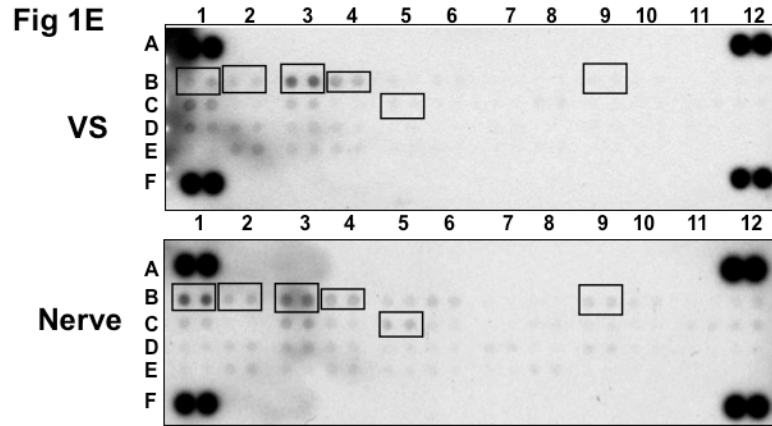
Figure 1A

	1	2	3	4	5	6	7	8	9	10	11	12
A	Positive control	Blank	Blank	Blank	Blank	Blank	Blank	Blank	Blank	Blank	Blank	Positive control
B	EGFR	ErbB2	ErbB3	ErbB4	FGFR1	FDFR2α	FGFR3	FGFR4	Insulin R	IGF-I R	Axl	Dtk
C	Mer	HGFR	MSPR	PDGFRα	PDGFRβ	SCFR	Flt-3	M-CSFR	C-Ret	ROR1	ROR2	Tie-1
D	Tie-2	TrkA	TrkB	TrkC	VEGFR1	VEGFR2	VEGFR3	MuSK	EphA1	EphA2	EphA3	EphA4
E	EphA6	EphA7	EphB1	EphB2	EphB4	EphB6	Negative Control	Negative Control	Negative Control	Negative Control	Negative Control	Blank
F	Positive control	Blank	Blank	Blank	Blank	Blank	Blank	Blank	Blank	Blank	Blank	Positive control

Figure 1B

Figure 1C

	1	2	3	4	5	6	7	8	9	10	11	12
A	Positive control	Blank	Blank	Blank	Blank	Blank	Blank	Blank	Blank	Blank	Blank	Positive control
B	EGFR	ErbB2	ErbB3	ErbB4	FGFR1	FDFR2α	FGFR3	FGFR4	Insulin R	IGF-I R	Axl	Dtk
C	Mer	HGFR	MSPR	PDGFRα	PDGFRβ	SCFR	Flt-3	M-CSFR	C-Ret	ROR1	ROR2	Tie-1
D	Tie-2	TrkA	TrkB	TrkC	VEGFR1	VEGFR2	VEGFR3	MuSK	EphA1	EphA2	EphA3	EphA4
E	EphA6	EphA7	EphB1	EphB2	EphB4	EphB6	Negative Control	Negative Control	Negative Control	Negative Control	Negative Control	Blank
F	Positive control	Blank	Blank	Blank	Blank	Blank	Blank	Blank	Blank	Blank	Blank	Positive control

Figure 1D

	1	2	3	4	5	6	7	8	9	10	11	12
A	Positive control	Blank	Blank	Blank	Blank	Blank	Blank	Blank	Blank	Blank	Blank	Positive control
B	EGFR	ErbB2	ErbB3	ErbB4	FGFR1	FDFR2α	FGFR3	FGFR4	Insulin R	IGF-I R	Axl	Dtk
C	Mer	HGFR	MSPR	PDGFRα	PDGFRβ	SCFR	Flt-3	M-CSFR	C-Ret	ROR1	ROR2	Tie-1
D	Tie-2	TrkA	TrkB	TrkC	VEGFR1	VEGFR2	VEGFR3	MuSK	EphA1	EphA2	EphA3	EphA4
E	EphA6	EphA7	EphB1	EphB2	EphB4	EphB6	Negative Control	Negative Control	Negative Control	Negative Control	Negative Control	Blank
F	Positive control	Blank	Blank	Blank	Blank	Blank	Blank	Blank	Blank	Blank	Blank	Positive control

Figure 1F

Figure 1. Phospho-RTK profiling in paired VS-nerve tissue specimens
(A) VS tumor/vestibular nerve pair from patient #1 expressed multiple RTKs (boxes). **(B)** Densitometry analysis showed a marked increase in pixel density of ErbB2 (B2) and ErbB3 (B3) as well as other RTKs in the tumor. **(C)** VS tumor/vestibular nerve pair from patient #2 demonstrated increased expression of ErbB3, which was quantified by densitometry analysis **(D). (E)** A third VS tumor/vestibular nerve pair demonstrated increased activation of ErbB3 (B3) in the tumor, which was quantified by densitometry analysis **(F)**.
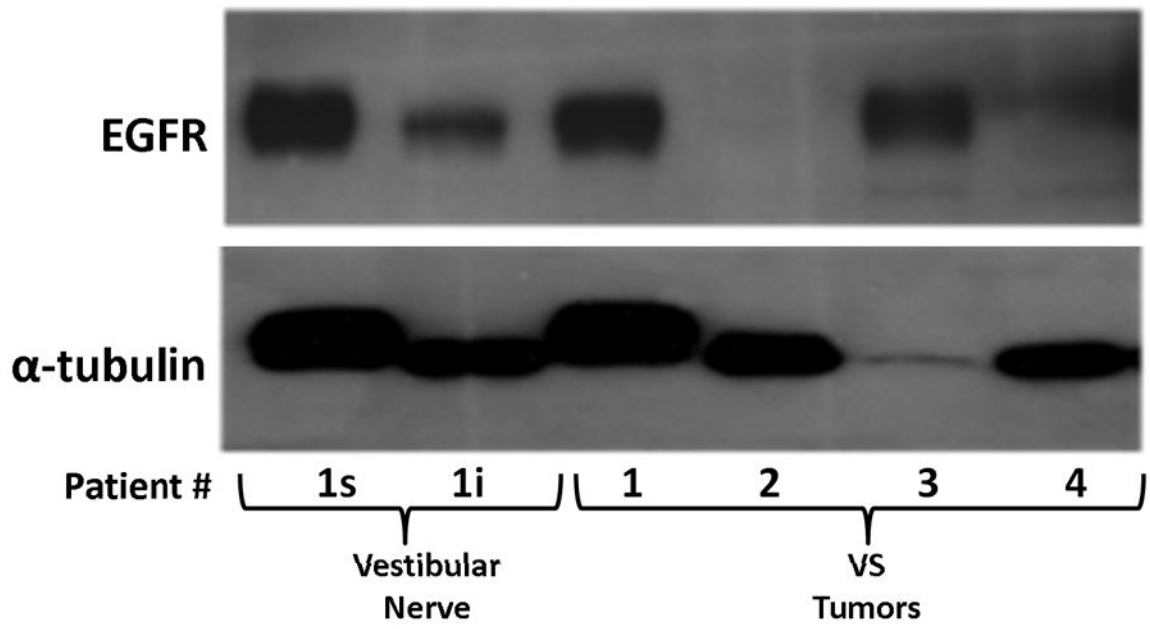
Figure 2. Detection of EGFR protein expression in VS tumor and vestibular nerve specimens
Western blot analysis using extracts from four VS tumors (1–4) and two branches of a
vestibular nerve were probed for EGFR protein. The superior (s) and inferior (i) branches of
the vestibular nerve were obtained from patient #1 who also had a VS (1).
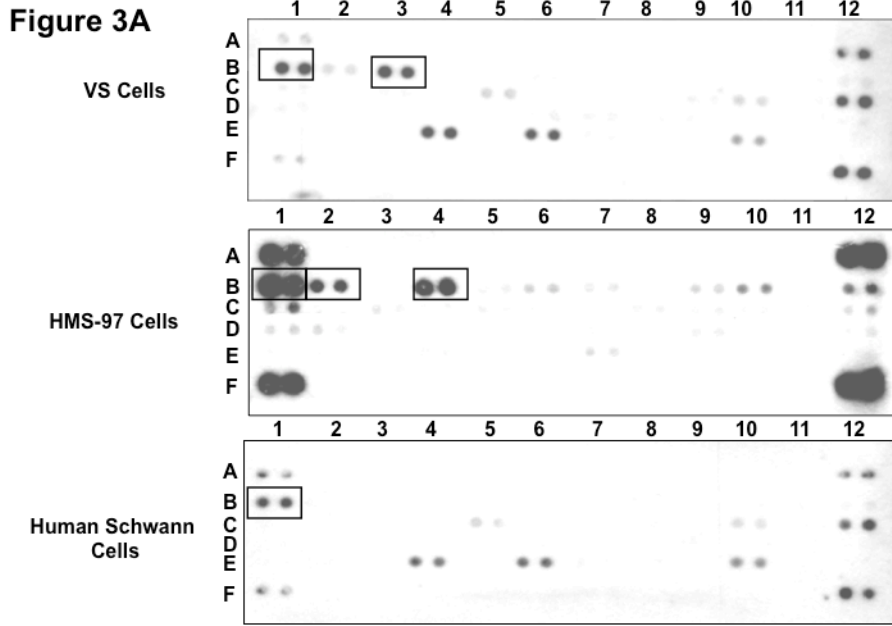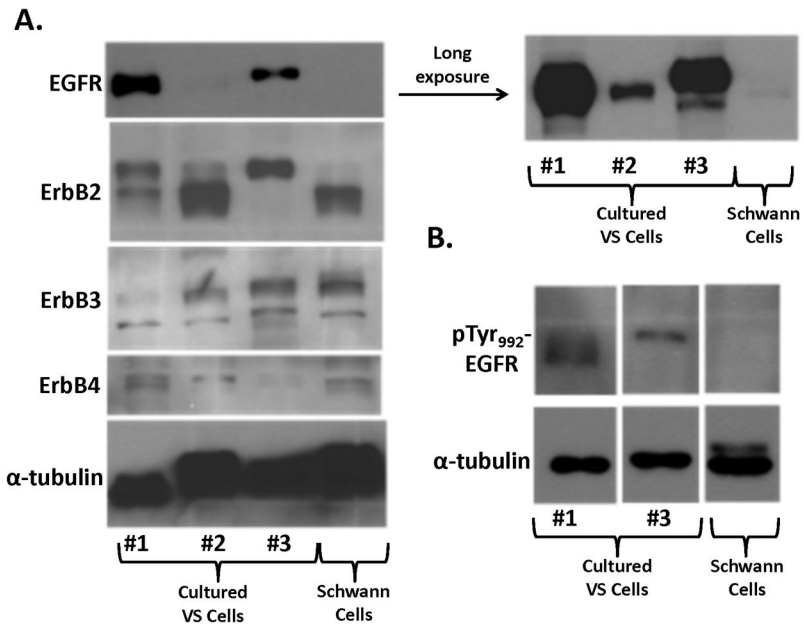
Figure 3A

Figure 3B

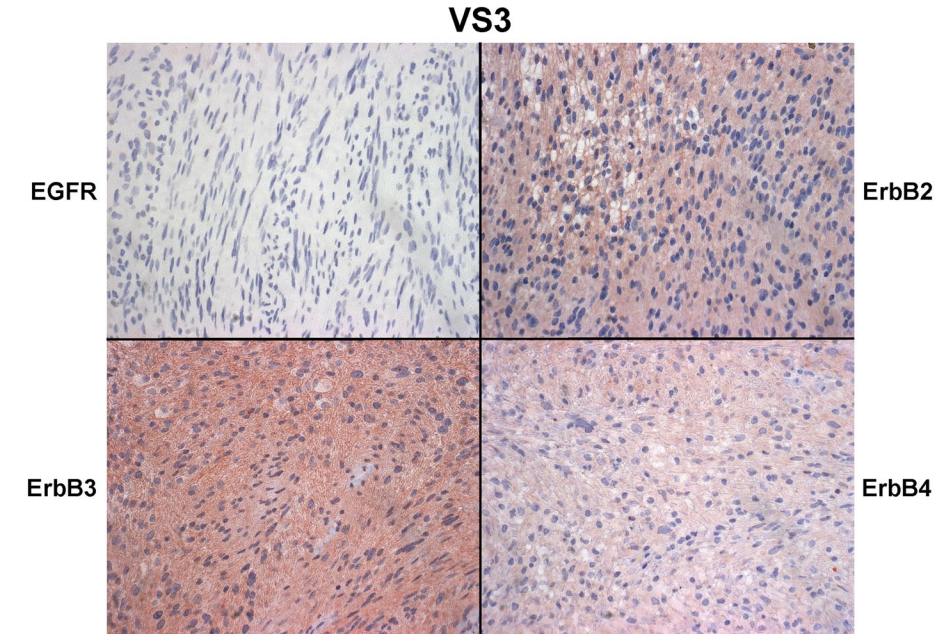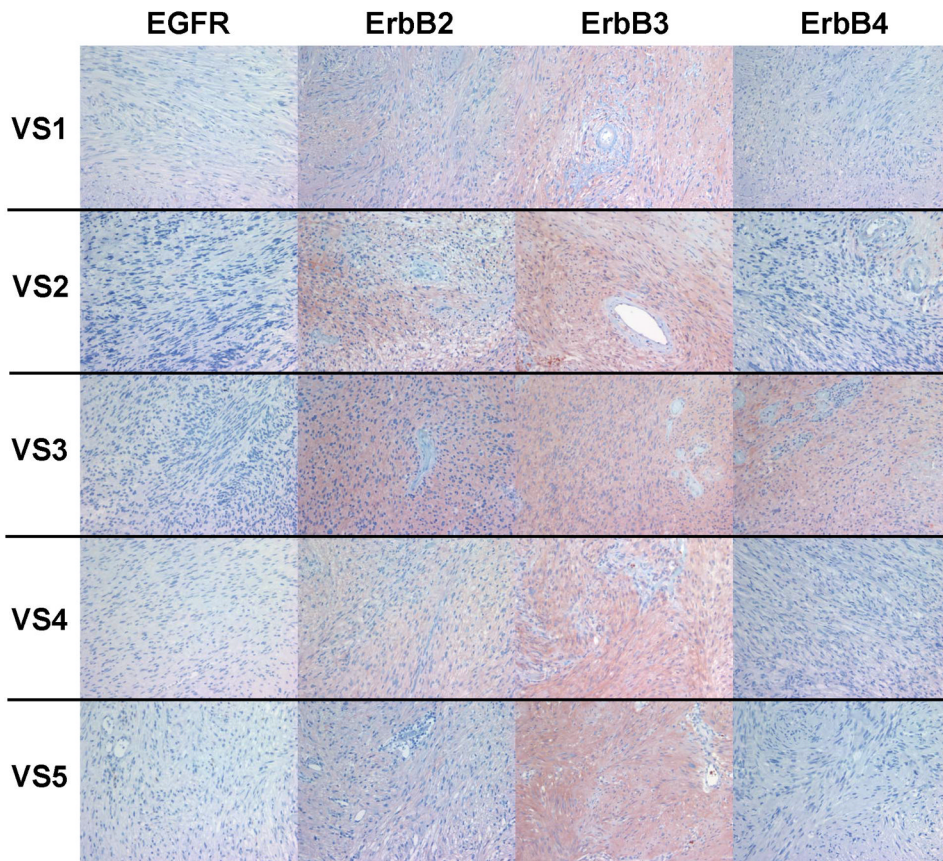|	1	2	3	4	5	6	7	8	9	10	11	12
A	Positive control	Blank	Blank	Blank	Blank	Blank	Blank	Blank	Blank	Blank	Blank	Positive control
B	EGFR	ErbB2	ErbB3	ErbB4	FGFR1	FDFR2α	FGFR3	FGFR4	Insulin R	IGF-I R	Axl	Dtk
C	Mer	HGFR	MSPR	PDGFRα	PDGFRβ	SCFR	Flt-3	M-CSFR	C-Ret	ROR1	ROR2	Tie-1
D	Tie-2	TrkA	TrkB	TrkC	VEGFR1	VEGFR2	VEGFR3	MuSK	EphA1	EphA2	EphA3	EphA4
E	EphA6	EphA7	EphB1	EphB2	EphB4	EphB6	Negative Control	Negative Control	Negative Control	Negative Control	Negative Control	Blank
F	Positive control	Blank	Blank	Blank	Blank	Blank	Blank	Blank	Blank	Blank	Blank	Positive control

Figure 3. Phospho-RTK profiling in cultured schwannoma and Schwann cells
Three primary VS cell cultures were established and used for preparing lysates for phospho-RTK array analysis according to Materials and Methods. A representative image of the array filter is shown. Normal Schwann cells were also prepared for the phospho-RTK array analysis and the image of the array filter is shown. Likewise, human malignant schwannoma HMS-97 cells were used in the analysis and the phospho-RTK expression file is shown **(A)**. The coordinates for phospho-RTK's are demonstrated **(B)**.

A.

EGFR

ErbB2

ErbB3

ErbB4

α-tubulin

#1 #2 #3

Cultured VS Cells

Schwann Cells

Long exposure →

#1 #2 #3

Cultured VS Cells

Schwann Cells

B.

pTyr₉₉₂⁻ EGFR
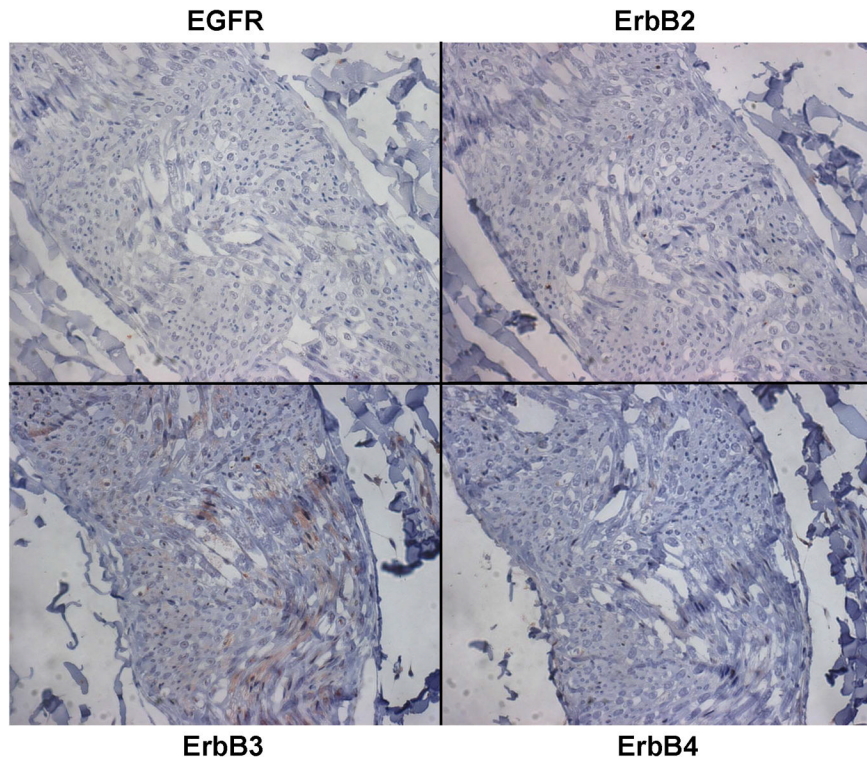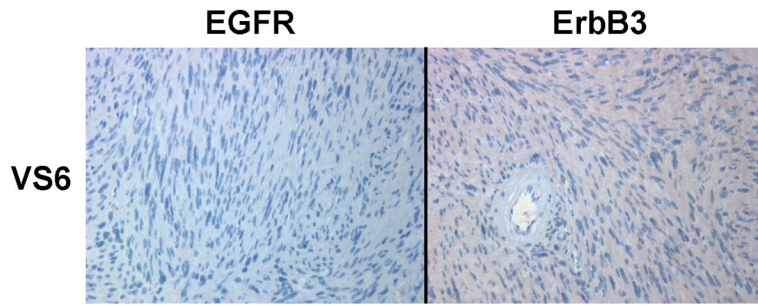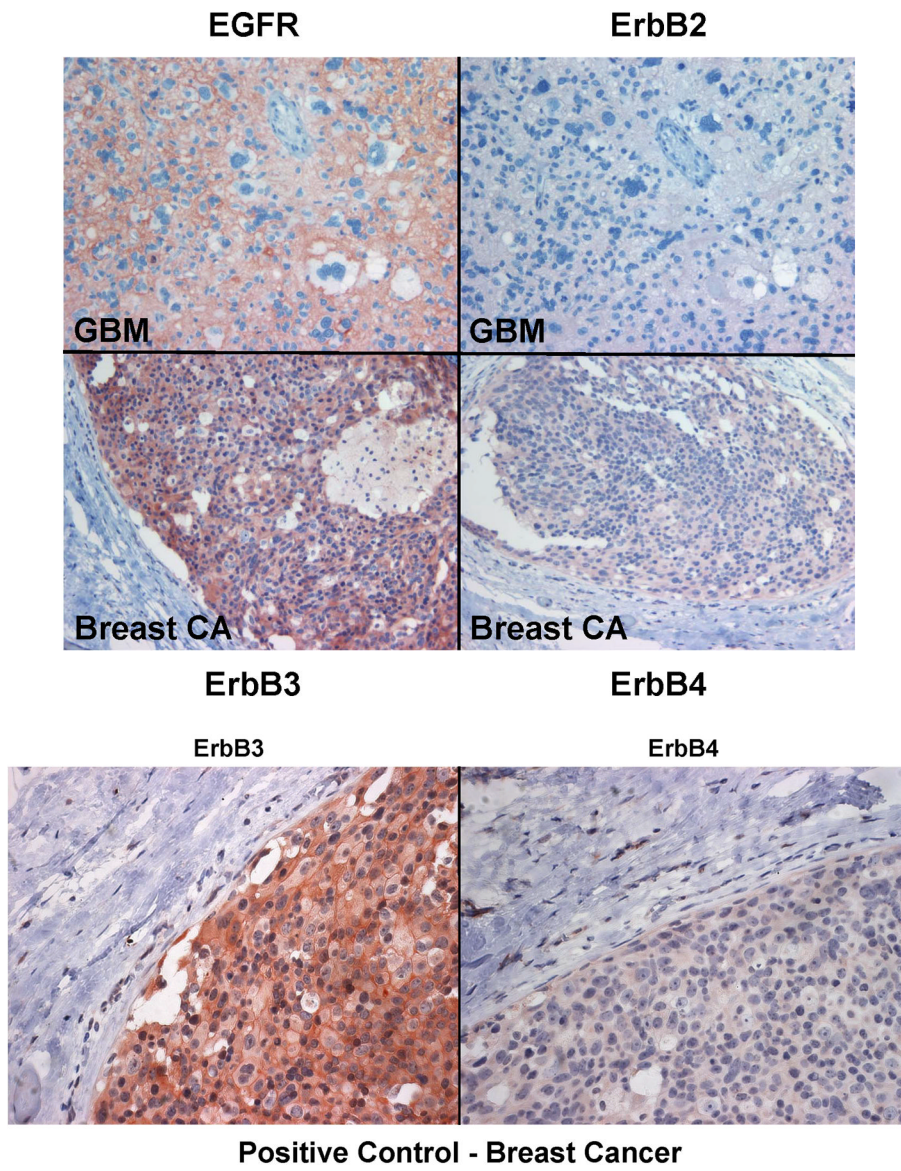
α-tubulin

#1 #3

Cultured VS Cells

Schwann Cells

Figure 4. Expression of various ErbB receptor proteins and phosphorylated EGF in cultured VS and Schwann cells

Protein lysates from three primary cultures of VS cells (#1–3) and one Schwann cell culture were used in Western blotting for total EGFR, ErbB2, ErbB3, and ErbB4 (A). A long exposure of the EGFR blot (shown in the right) revealed that normal Schwann cells expressed a low level of EGFR protein compared with strong expression in cultured VS cells. A similar Western blot was performed for phospho-EGFR expression in cultured VS and Schwann cells **(B)**.
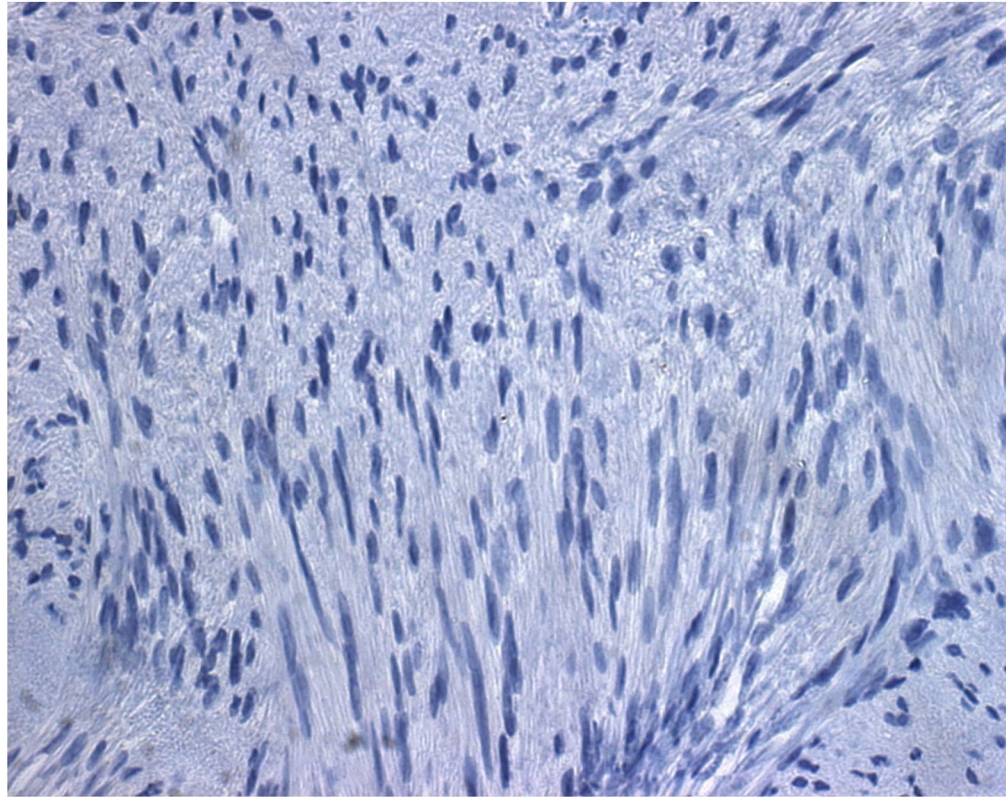
EGFR **ErbB3**

VS6

EGFR **ErbB2**

ErbB3 **ErbB4**

EGFR　　　　　**ErbB2**

ErbB3　　　　　**ErbB4**

Positive Control - Breast Cancer

Negative Control

Figure 5. Immunohistochemistry analysis of VS tumor sections for ErbB protein expression
Sections of six VS tumors were stained for expression of various ErbB members. Representative images of five VS tumor tissues immunostained for various ErbB members were shown **(A)**. High-magnified (400x) images of stained VS tumor #3 were illustrated **(B)**. A sixth VS tumor was also stained for EGFR and ErbB3 **(C)**. Sections of normal sciatic nerve were also stained for expression of various ErbB proteins **(D)**. Glioblastoma and breast carcinoma were used as positive controls for EGFR/ErbB2 and Erb3/Erb4, respectively **(E)**. High-magnified (400x) images of beast cancer tissues stained with ErbB3 and ErbB4 antibodies were also shown **(F)**. A VS tumor section subjected to immunostaining procedures but without the primary antibody was used as a negative control **(G)**.
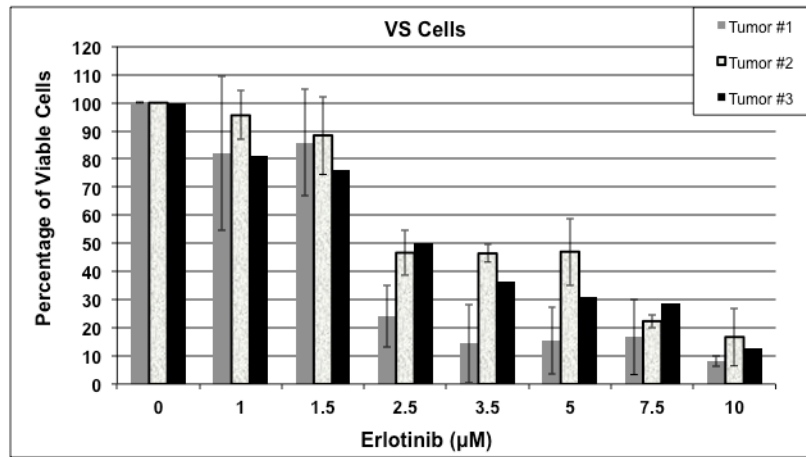
Figure 6A

VS Cells

Legend: Tumor #1, Tumor #2, Tumor #3

Y-axis: Percentage of Viable Cells
X-axis: Erlotinib (μM)

Figure 6B

HMS-97 Cells

Y-axis: Percentage of Viable Cells
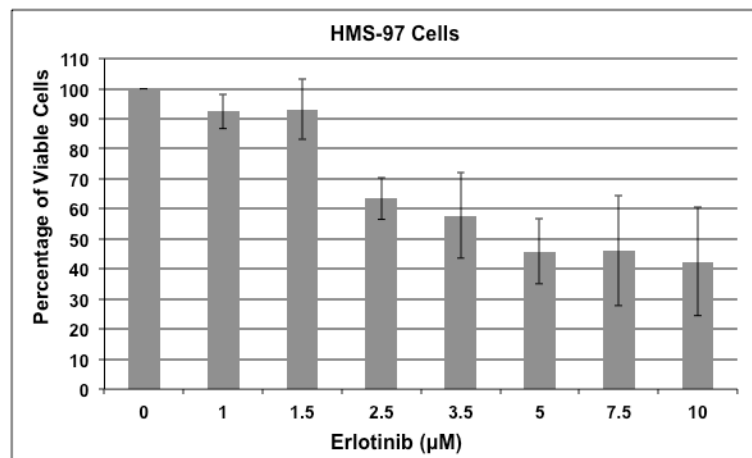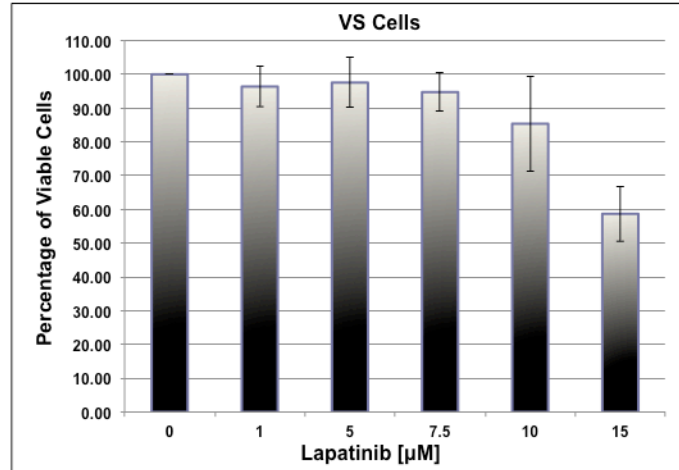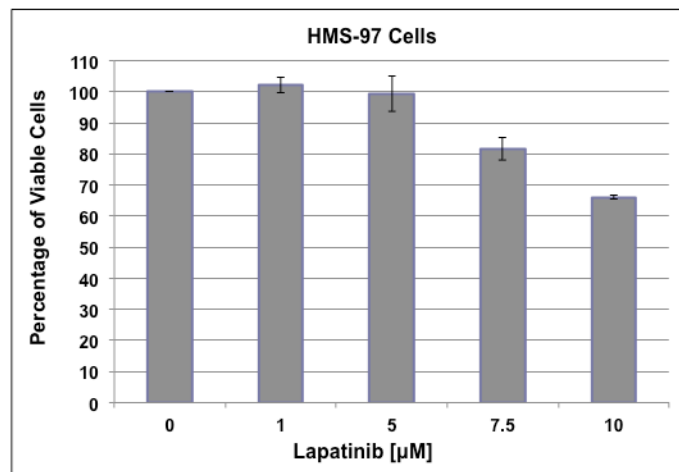X-axis: Erlotinib (μM)
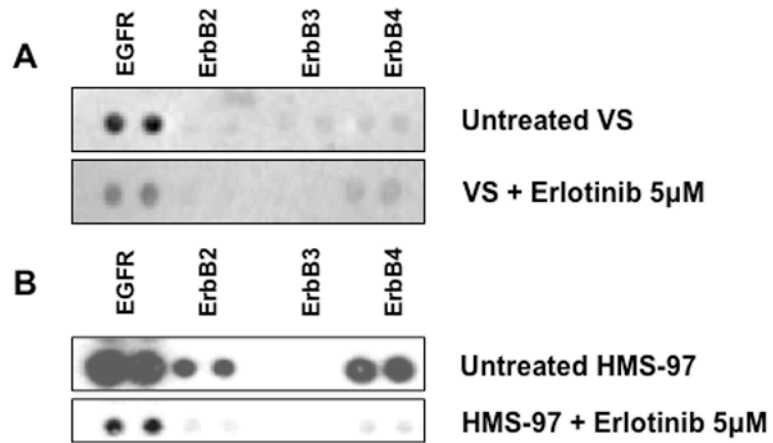
Figure 6C

Figure 6D

Figure 6. Growth inhibition of primary VS and malignant schwannoma HMS-97 cells by Erlotinib and Lapatinib
Three VS cultures (**A**) and HMS-97 cells (**B**) were treated various doses of Erlotinib and cell proliferation was determined using MTS assays. Similarly, cultured VS (**C**) and HMS-97 cells (**D**) were treated with the indicated doses of Lapatinib and assayed for cell proliferation.

Figure 7. Decreased expression of phospho-ErbB receptors in Erlotinib-treated VS and HMS-97 cells
Protein extracts from untreated and erlotinib-treated VS (**A**) or HMS-97 cells (**B**) were hybridized with phospho-RTK arrays as described in Methods.

Table 1

Relative expression levels of phospho-RTKs in VS/vestibular nerve pairs. The pixel densities from figures 1B, 1D, and 1F of each phospho-ErbB receptor for each tumor were compared to their respective paired nerve receptors and ratios was calculated. Higher relative phospho-RTK expression in vestibular nerves resulting in negative ratios were not included in this table.

Ratio between each VS VN Pair			
Tumor	1	2	3
p-EGFR	1.02	–	–
p-ErbB2	6	–	–
p-ErbB3	12.8	2.3	1.9
p-ErbB4	–	–	1.1

Table 2

Characteristics of VS tumors examined with immunohistochemical staining.

Tumor	Type	Size (cm)
1	NF2	1.8
2	Sporadic	2.1
3	Sporadic (Cystic)	2.1
4	Sporadic	2.2
5	Sporadic (Cystic)	2.3